Agile RF Systems for On-Demand Wireless Power Transfer

Title: Agile RF Systems for On-Demand Wireless Power Transfer

Authors: Tommaso Tiberi, Lorenzo Bastia, Alessandra Costanzo, Diego Masotti

Tommaso Tiberi (tommaso.tiberi@unibo.it), Lorenzo Bastia (lorenzo.bastia3@unibo.it), Alessandra Costanzo (alessandra.costanzo@unibo.it; ORCID 0000-0001-5073-000X), and Diego Masotti (diego.masotti@unibo.it; ORCID 0000-0001-5340-2781) are with the Alma Mater Studiorum University of Bologna, Department of Electrical, Electronic and Information Engineering – Guglielmo Marconi – Bologna, ITALY.

1. Introduction

Wireless power transfer (WPT) is becoming a crucial and demanding technology in moder wireless systems. In recent years, many research activities about far-field WPT have been conducted to face the various obstacles and challenges presented by this type of wireless system. A block-scheme representation of a generic far-field WPT system is shown in Fig 1.

The efficiency of the WPT system is a crucial parameter to assess the reliability of the entire wireless link. According to the schematic in Fig. 1, the total efficiency results from the combination of several factors, indeed it can be expressed as:

$$\eta_{TOT} = \frac{P_{IN}}{P_{BIAS}} \cdot \frac{P_{ANT}}{P_{IN}} \cdot \frac{P_{TX}}{P_{ANT}} \cdot \frac{P_{RX}}{P_{TX}} \cdot \frac{P_{DC}}{P_{RX}} \cdot \frac{P_{HARV}}{P_{DC}} = \tag{1}$$

$$= \eta_{osc} \cdot \eta_{amp} \cdot \eta_{ant} \cdot \eta_{link} \cdot \eta_{rect} \cdot \eta_{boost}$$

Where: η_{osc} is the efficiency of the oscillator defined as the power that it provides at the input of the power amplifier P_{IN} with respect to the DC power P_{BIAS}; η_{amp} is the efficiency of the power amplifier defined as the ratio between the power at the input of the transmitting antenna P_{ANT} and the power at the input of the power amplifier P_{IN}; similarly the antenna efficiency η_{ant} is the ratio between the power radiated by the transmitting antenna P_{TX} and the power at its input; η_{link} is the efficiency of the wireless link between the transmitter and the receiver and it is built by the ratio between the power collected by the receiving antenna P_{RX} and the power radiated by the transmitting antenna. This efficiency term accounts for the propagation impairments (e.g. losses) through the wireless channel; η_{rect} is the efficiency of the rectifier connected to the receiving antenna, and it is obtained by dividing the DC power P_{DC} at the rectifier output with respect to the RF power P_{RX} at its input; finally, η_{boost} is the efficiency of the DC-DC converter that takes the DC power at the rectifier output and provides an output power P_{HARV} to be collected in a storage capacitor.

At the transmitting side, the oscillator, amplifier and antenna efficiencies can easily reach values significantly greater than 50 % (around 80 % in the low-GHz range, down to 60 % above 10 GHz). Regarding the receiver side, the RECTENNA RF-to-dc efficiency has reached its limits: in environmental energy harvesting scenarios with available power levels around [-20 – -10] dBm the efficiency can be 30-50 %, reaching 60-70 % for higher power levels ([0 – 10] dBm). A less critical block is the dc-to-dc converter, where an efficiency around 90 % can be guaranteed. On the other hand a major issue of a WPT link working in far-field conditions is the lack of effective RF-to-RF efficiency of the wireless channel (η_{link}), due to the long distance between transmitter and receiver. This physical limitation can be somehow counteracted by designing advanced radiating architectures that are able to boost the power transfer efficiency (dc-to-dc efficiency) of the whole system, minimizing the

 Doi: 10.1109/MMM.2025.3604719

impact of the RF link. In this work, a review on two key technologies, which could play, to the authors' opinion, a strategic role in WPT applications, named Frequency Diverse Arrays (FDA) and Time Modulated Arrays (TMA) is proposed. They represent two groups of radiating systems that have been studied and developed significantly in the last decades due to their interesting and unique radiating capabilities. In particular, these types of array show a great level of pattern reconfigurability, in terms of beamforming and beam-steering, while preserving a rather simple architecture compared with the state-of-the-art. For this reason, they are considered promising RF systems for on-demand wireless power transfer. The adjective "on-demand" refers to the possibility to adapt almost in real-time the configuration of the array, to choose and modify its radiating behavior, according to the application requirements. In a WPT scenario these requirements could be given by the number and position of the devices to be energized in a given environment.

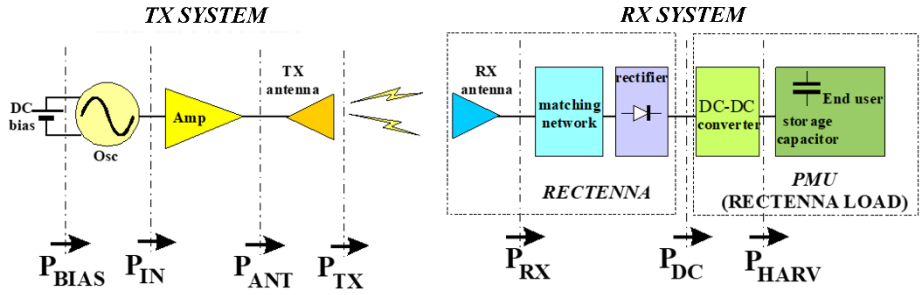

Fig. 1. Block-scheme of a far-field WPT system.

2. Frequency Diverse Arrays

FDAs have been the subject of many research studies over the last decades. Their main feature is the frequency diversity among the signals radiated by each array element, that enables interesting beam steering and beamforming capabilities [1]. The intermodulation of signals at slightly different frequencies generates a particular S-shape beam pattern in the range-angle plane, characterized also by a peculiar time dependency [2],[3]. According to the excitation signal regime, two classes of FDA systems are recognized: continuous wave (CW) FDA and pulsed FDA.

2.1. CW Frequency Diverse Arrays

CW FDAs are based on a continuous signal (e.g. cosine waveform) radiated by each array element. The standard and easiest FDA system is composed by a linear 1-D array of M elements as depicted in Fig. 2(a). A linear and progressive frequency offset Δf is introduced among the antennas, such that the operating frequency of the m^{th} antenna element is given by:

$$f_m = f_0 + m\Delta f \tag{2}$$

In this case, the resulting array beam pattern, shown in Fig. 2(b), is characterized by a time-angle coupling [4] as can be evinced from its S-shape.

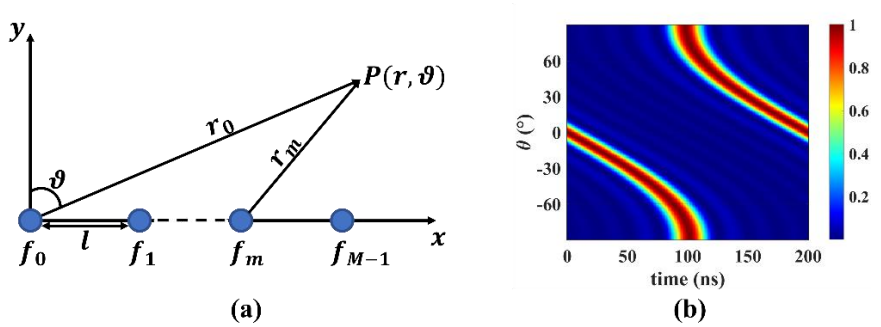

Fig. 2. Linear (1-D) frequency diverse array: (a) array layout, (b) normalized beam pattern.

The main property of this system is the automatic and real-time steering of the radiated beam as can be evinced in Fig. 2(b). This behavior is achieved without employing additional hardware, such as phase shifters employed in phased arrays, but it simply results from the introduction of a frequency diversity among the array elements [5]. In particular, the FDA beam pattern exhibits a time (and space) periodicity that is inversely proportional to Δf: the higher is the frequency offset, the lower is the scanning time of FDA, and vice versa [6] (in Fig. 2(b) the time periodicity is 200 ns, corresponding to $1/\Delta f$ when $\Delta f = 5\ MHz$) The time-angle dependency, combined with the automatic beam-scanning capabilities of the beam pattern, make CW FDA an interesting solution in radar applications [7-10]. However, the strict dependency between time and angle introduces some issues for those applications, such as WPT, in which a full control of the radiation is mandatory. Indeed, for WPT purposes a time-angle decoupling of the FDA beam pattern must be pursued to control and select a desired radiation direction only. In the last years, many efforts have been spent by the research community in this direction, following different approaches. A first strategy consists of the optimization of the frequency offset Δf between the FDA signals. For example, by introducing a logarithmic step instead of a linear one, the FDA beam pattern tends to assume an almost elliptical shape pattern [11],[12], highlighting the possibility to better control the system's radiation. A similar result is achieved by applying a symmetric (linear) frequency distribution to the array elements [13],[14]. An example of the normalized beam pattern of a linear FDA with logarithmic frequency offset and symmetric frequency offset is shown in Fig. 3(a) and Fig. 3(b), respectively.

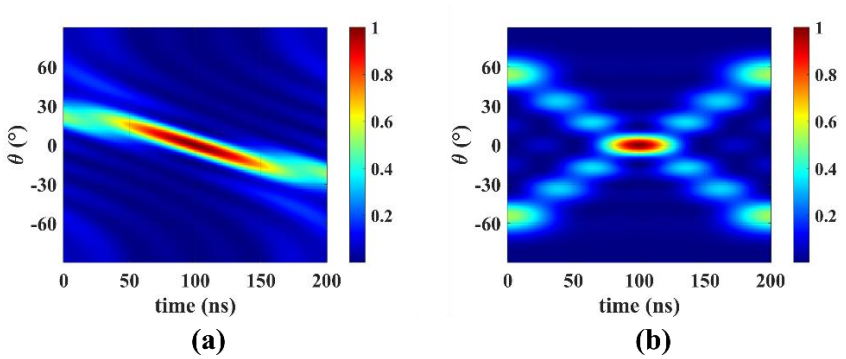

Fig. 3. Normalized beam pattern of a linear FDA with (a) logarithmic frequency offset, (b) symmetric frequency offset.

Successively, it has been proved that by extending the FDA principle to planar 2-D arrays, a very precise dot-shape pattern is obtained still preserving a linear Δf value [15]. In this context, the exploitation of array topologies with circular geometry has demonstrated to be the best solution [16-18], compared to square/rectangular layouts [19], since the generated beam preserves its symmetry across all the azimuthal planes and the S-shape is completely removed. For example, by considering a 24-element circular array,

organized in $M = 3$ rings, each one composed by $N = 8$ elements, the normalized FDA beam pattern according to two different frequency distribution rules can be derived. Indeed, frequency diversity can be applied among the N spokes of the array (radial FDA), resulting in the beam pattern shown in Fig. 4(a), or among the M rings (concentric circular FDA), thus providing the beam pattern in Fig. 4(b).

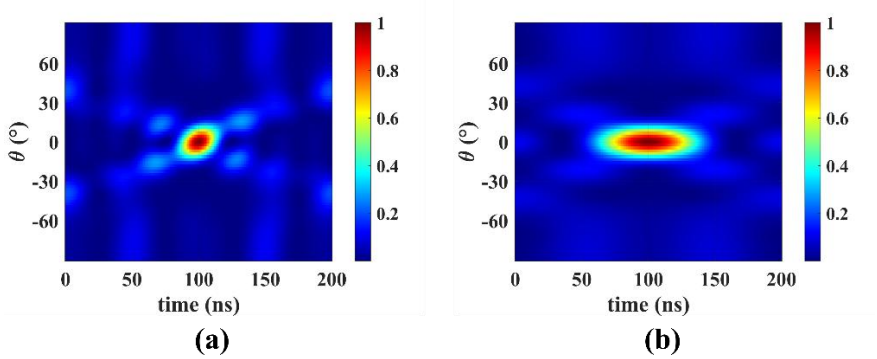

Fig. 4. Normalized beam pattern of a 24-element circular FDA with $M = 3$ rings, and $N = 8$ spokes: (a) radial FDA, (b) concentric circular FDA.

However, all these alternatives introduce a significant level of complexity, either for the signal generation if a non-linear frequency distribution rule is adopted, or for the array design and excitation if a large number of elements deployed in a planar layout is used. Moreover, in those circumstances the beam pattern reconfigurability is rather low, and once the system is designed, beam-steering is possible only resorting to phase shifters.

2.2. Pulsed Frequency Diverse Arrays

A powerful alternative to solve this problem is to introduce a pulsed regime, to select on demand the desired direction(s) of radiation [20]. In this scenario a very simple layout is needed, involving a linear array with linear frequency shift Δf. Replacing the CW signals with pulsed waveforms, a dot-shaped pattern is achieved, thus resolving the time-angle coupling phenomenon. The total radiated signals can be expressed as:

$$x(t) = \sum_{m=0}^{M-1} x_p(t) \cdot e^{j2\pi f_m t} \tag{1}$$

where $x_p(t)$ is the pulse adopted for the modulation of the carrier, M is the number of array elements, and f_m is the frequency of the m^{th} signal radiated by the m^{th} antenna. The pulse delay and its duty cycle play a crucial role as design parameters to define the radiation direction and the spot accuracy, respectively. In particular, the pulse delay can be selected on demand to perform beam steering without the need of any phase shifter. An example of such radiating behavior can be appreciated by observing Fig. 5, in which the normalized beam pattern for a linear FDA of $M = 8$ elements, carrier frequency $f_0 = 1.8\ GHz$, $\Delta f = 5\ MHz$, whose signals are modulated by a rectangular pulse with duty cycle $d = 0.1$ and delay $\tau = 70\ ns$ is represented.

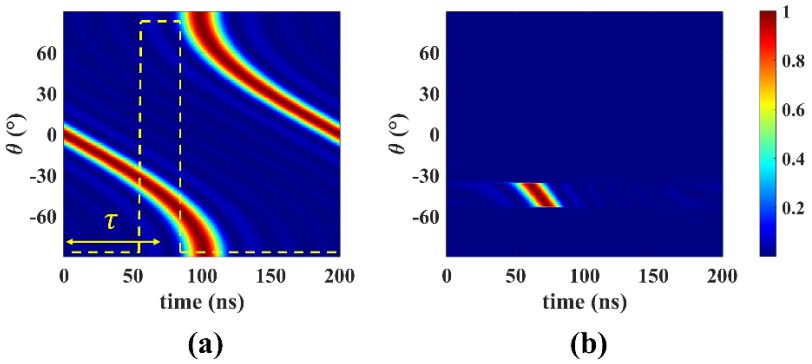

Fig. 5. Normalized beam pattern of (a) CW FDA with superimposed pulse (yellow dashed line), (b) pulsed FDA.

The effect of the pulse modulation on the FDA beam pattern is well-visible in Fig. 5(b): the original S-shape is replaced in favor of a dot-shape radiation centered around $\theta = -45°$.

As stated in [6], the choice of Δf defines univocally the time periodicity of any FDA radiation pattern, being equal to $1/\Delta f$. If a unique pulsed sequence is designed within a certain FDA period (accordingly to the case shown in Fig. 5), a single spot pointing in a predefined target direction is generated. However, by properly combining multiple (not overlapping) ON-OFF sequences, multiple spots are simultaneously generated in different directions according to the delay value of each control pulse. This single- and multi-beam capability via pulsed FDA has been experimentally demonstrated for the first time in [21] with a simple four-finger series-fed patch array operating at 1.9 GHz, and the corresponding results are recalled in Fig. 6. In particular, a single-beam configuration pointing at $\theta = -30°$ is shown in Fig. 6(a), whereas a double-beam radiation pointing at $\theta = -20°$ and $\theta = 30°$ simultaneously, is generated in Fig. 6(b), by combining a couple of delayed control sequences.

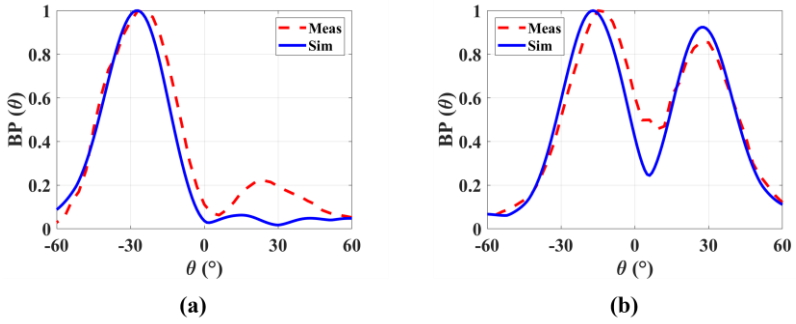

Fig. 6. Normalized beam pattern for (a) single-beam pulsed FDA, (b) multi-beam pulsed FDA. [21]

A picture of the indoor measurement set-up is reported in Fig. 7: in order to ensure the coherency of the M frequency-diverse radiated signals, a Software Defined Radio (Xilinx RFSoC ZCU111) is required for the FDA signals generation.

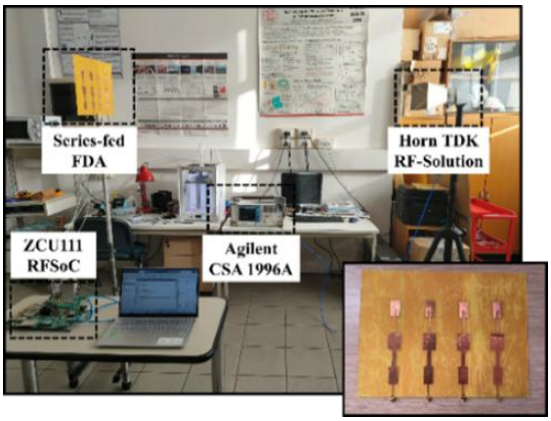

Fig. 7. Indoor laboratory set-up for pulsed FDA measurements. [21]

The FDA architecture combined with a pulsed excitation regime (i.e. pulsed FDA) is currently the best solution to resolve the time-angle coupling phenomenon, and easily allows single-beam and multi-beam generation according to the target radiation direction(s). This high level of reconfigurability achieved with a simple and precise time-control makes the pulsed FDA system a valuable solution for WPT applications.

2.3. Harmonic analysis of pulsed FDA

The control strategy based on a pulsed waveform described in section 2.2 is responsible for the generation of infinite harmonic products due to the intermodulation of the FDA carriers f_m with the control frequency f_p of the ON–OFF sequences. Therefore, the spectrum of the radiated signals inherently contains infinite harmonic terms, due to the pulse modulation: such scenario is depicted in Fig. 8 in the case of four different radiated tones (as in the previous measurement).

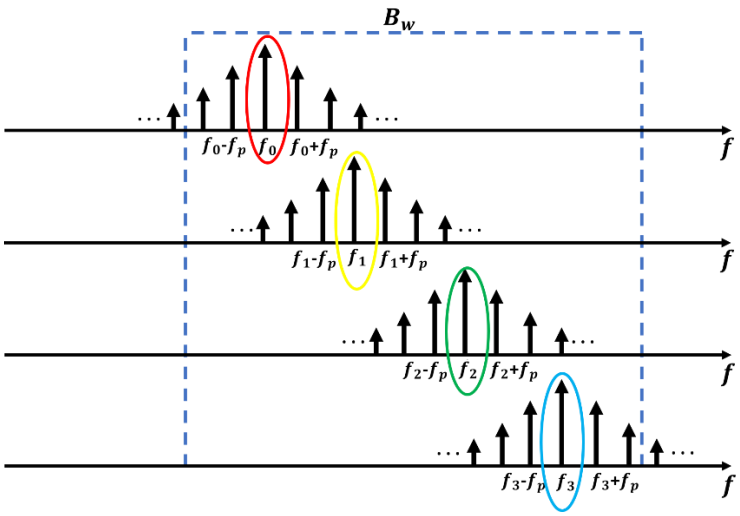

Fig. 8. Spectrum of a 4-element pulsed FDA. The carriers are highlighted with different colors [22].

Those harmonic contributions must be handled to avoid excessive power loss outside the operating bandwidth of the system B_w. Indeed, a study on the spectral characteristics of the pulsed FDA waveforms is mandatory. This analysis was exhaustively conducted for the first time in [22]. It has been proved that, differently from a communication scenario where the harmonic tones must be spread outside B_w to avoid in-band interference

and distortion (resulting in huge levels of power loss), the generated harmonics can be favorably exploited for WPT purposes, thus minimizing the out-of-band power loss and preserving the effectiveness of pulsed FDA for WPT applications. To validate the theoretical study, an experimental activity was conducted, comparing different shapes of the driving pulse: rectangular, triangular and raised cosine (RC). A 4-monopole linear array was used as transmitter with $f_0 = 1.8\ GHz$ and $\Delta f = 5\ MHz$. The power loss curves, function of the available bandwidth B_w, are shown in Fig. 9.

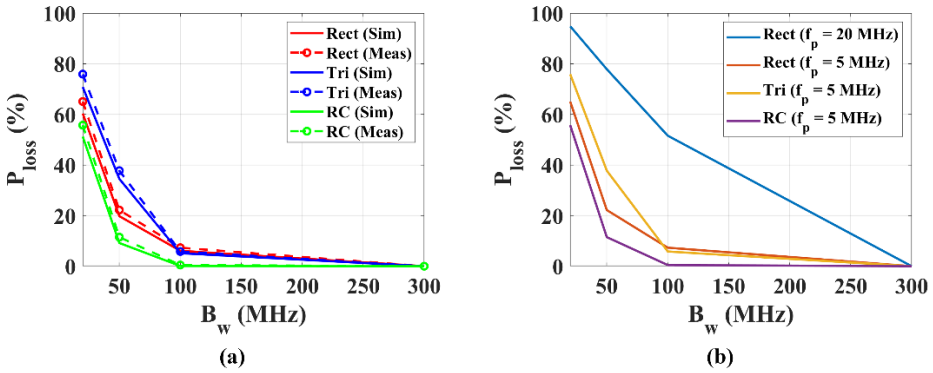

Fig. 9. (a) Simulations (continuous line) and measurements (dashed line) results of power loss for different pulse waveforms. (b) Measured power loss curves [22].

Observing Fig. 9(b) it is evident that by choosing a pulse repetition frequency $f_p = 20\ MHz$, required for communication purposes, the power loss levels are significantly high, and most of the available power is lost on the side-band harmonics. Whereas, for WPT it is possible to reduce the harmonic spacing ($f_p = 5\ MHz$) and consequently minimize the power loss. Furthermore, by comparing the different pulse shapes with the same value of $f_p = 5\ MHz$, the pulsed FDA based on RC pulse provides the highest power loss reduction.

3. Time Modulated Arrays

In a TMA architecture each antenna element of the array radiates the same RF signal modulated by a switch through a periodic pulse with repetition frequency f_p and periodicity $T_p = 1/f_p$ [23],[24]. Differently from the pulsed FDA previously described, each switch has now its own periodic pulse (with duty cycle and rise instant as additional new degrees of freedom). Due to the time-based control, TMAs own the unique capability of generating a multi-harmonic radiation pattern. Therefore, the radiation occurs at the radio frequency (RF) carrier f_0, and at the harmonic frequencies $f_{\pm h} = f_0 \pm hf_p$, where h is the harmonic index [25],[26]. The ON-OFF status of the switches allows an almost infinite number of driving sequences to be chosen in the multi-harmonic radiation patterns synthesis phase. In particular the duty cycle and delay of the pulse act on the amplitude and phase of the harmonics, respectively.

3.1. TMA architecture for WPT

In principle, the TMA architecture is extremely simple since the beamforming capability of the harmonic patterns is synthetized without employing additional hardware components such as phase shifters. However, if highly directive applications are envisaged, such as selective and precise WPT, a huge number of radiating elements is required, and the design of the TMA control network becomes a cumbersome task. In fact, by considering a planar array of MxN number of elements, in principle one switch per each antenna (MxN in total) would be required to implement the time-modulated scheme. To face this problem, in [27] a planar multi-spoke TMA with agile control of the time-based network has been proposed. The multi-layer array layout, shown in Fig. 10, is based on $N = 8$

spokes, each one made of $M = 3$ series-fed patch antennas operating at 2.45 GHz.

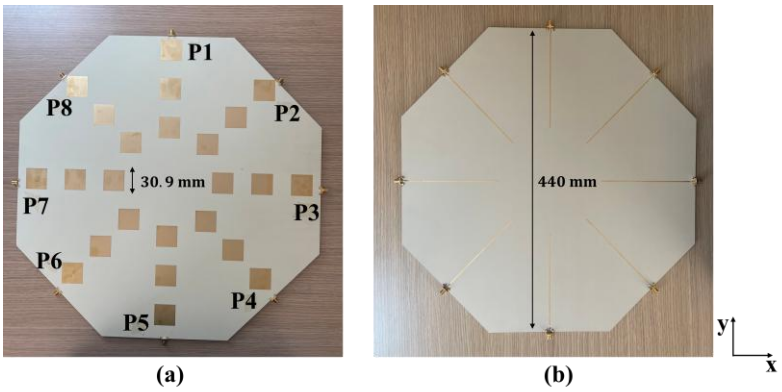

Fig. 10. Planar multi-spoke array: (a) front view, (b) back view. [27]

In this way, despite the high number of radiators ($MxN = 24$) involved, each spoke can be controlled by a single RF switch (instead of employing one switch per antenna element), thus significantly reducing the complexity of the time-based architecture. Therefore, with only $N = 8$ switches applied at the spokes input ports, the entire 24-element array can be controlled with the TMA principle. The total signal radiated by this TMA system is written as:

$$y(t) = \sum_{n=0}^{N-1} \sum_{h=-\infty}^{h=+\infty} C_h^n e^{j2\pi(f_0+hf_p)(t-\tau_n)} \tag{2}$$

where C_h^n and τ_n are the amplitude coefficients and delay of the pulse wave controlling the n^{th} element. In [27] a MATLAB example of multi-goal optimization of the driving sequences controlling the array ports is done, in such a way to maximize, in the horizontal scanning plane, the amplitude of the first order harmonic ($h = 1$) in a target direction ($\vartheta_t = 20°, \varphi_t = 0°$), while reducing the impact of the superior harmonics. The corresponding results are shown in Fig. 11. This represents just an example of a use case scenario in which the goal is to exploit the radiation of the fundamental and first order harmonics only, mitigating the interference coming from the harmonics of order greater or equal than 2. However, there could be other conditions in which the higher order harmonics are exploited as well.

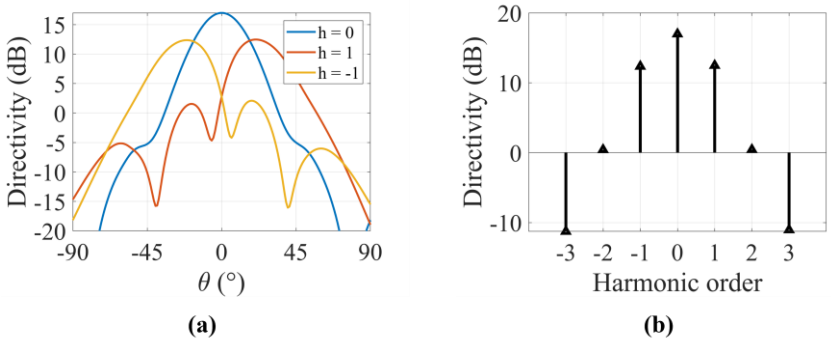

Fig. 11. (a) directivity pattern at fundamental tone ($h = 0$) and first harmonics ($h = -1, +1$), (b) maximum directivity at different harmonics. [27]

Furthermore, the exploitation of a highly symmetric layout with circular symmetry enables 2D beam steering features (i.e., scanning on a plane $\varphi_t \neq 0°$) simply playing with the order of control of the input ports. Overall, the agile switching control network together with the benefits of the array circular symmetry make the radial TMA an interesting candidate for highly selective and reconfigurable WPT applications.

3.2. TMA architecture for localization

The positioning problem is a very important part of a two-step procedure that includes a preliminary localization of objects such as tags/sensors distributed in a certain environment followed by the wireless powering of the detected targets. To this aim, the use of a single radiating architecture capable of supporting both applications and to be easily reconfigured from one task to the other is crucial. Indeed, the TMA principle applied to a two-element array, for direction finding applications, has been deeply investigated in the literature [28-30]. In particular, the multi-harmonic generation of a TMA can be favorably exploited for localization by relying on the radar monopulse principle [31]. The main idea is to exploit the strategic correspondence between the harmonic patterns and the observation direction as a function of the adopted TMA control sequences. Indeed, the radial TMA presented in section 3.1 as a powerful solution for WPT, was also studied and configured for direction finding purposes [32]. This localization approach requires a low directive beam pattern with reduced side lobes at the fundamental frequency, to avoid detection uncertainties. Therefore, only two adjacent spokes (out of eight in total) are used. It has been proved that, by piloting the two array ports with specific control sequences that have a relative delay $\Delta\tau$, the first-order harmonics ($h = \pm 1$) are steered in symmetric directions with respect to the fundamental one ($h = 0$), as shown in Fig. 12.

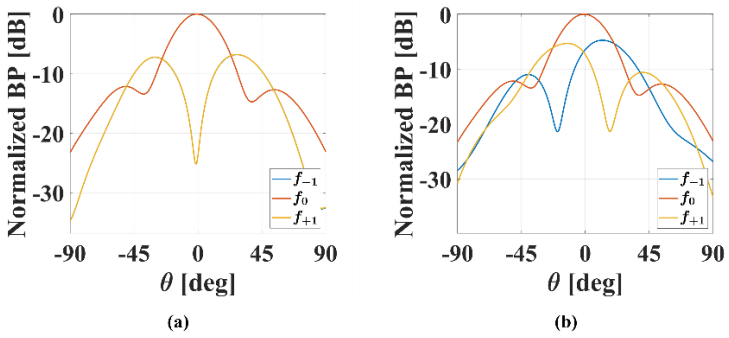

Fig. 12. Normalized beam pattern on the plane $\phi = 0°$: (a) $\Delta\tau = T_p/2$ (f_{-1} and f_{+1} are superimposed), (b) $\Delta\tau = T_p/4$ [32].

This implies that each direction in space corresponds to a distinct and unique harmonic spectrum, as reported in Fig. 13, and the localization approach is based on the correspondence between harmonics power and the observation direction. A proof-of-concept of this harmonic-based localization method was conducted as well in [32], based on the analysis of the received TMA signal. A good agreement between simulated and measured results was found (as visible from Fig. 13), highlighting the practical effectiveness of the proposed TMA solution for direction finding applications.

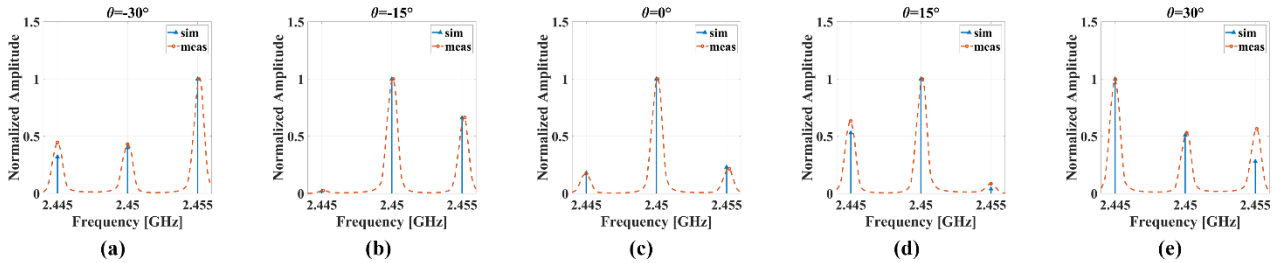

Fig. 13. Simulated and measured normalized amplitude spectrum on the plane $\phi = 0°$ for (a) $\theta = -30°$, (b) $\theta = -15°$, (c) $\theta = 0°$, (d) $\theta = 15°$, (e) $\theta = 30°$. [32]

4. Comparison with other systems for WPT

In sections 2 and 3 two different architectures have been described as innovative solutions to develop an efficient far-field WPT system. However, interesting alternatives are available in the literature, and among them, retrodirective antenna arrays (RDA) represent a promising system for joint tracking and powering operations. The retrodirectivity principle applied to an array with dual-frequency, dual-polarization was proposed in [33], in particular the proposed RDA works at 3.8 GHz with right-hand circular polarization in reception and transmits at 5.8 GHz with left-hand circular polarization. Moreover, in [34] a novel circularly polarized (CP)-RDA for WPT applications has been designed, by exploiting subarrays in transmission, to reduce the number of active components needed for the RDA and therefore minimizing the cost. A schematic of the architectures proposed in [33],[34] is shown in Fig. 14(a) and Fig. 14(b), respectively. The general idea of these systems is to exploit the incoming low-power pilot signals from the user to track its position and subsequently transfer high-power in the same and proper direction. In both cases, the use of a circular polarization both in transmission and in reception enables higher flexibility in the orientation of the device to be energized, and could be beneficial in presence of mobility (e.g. mobile phone charging). Furthermore, two orthogonal polarizations, right-hand circular polarization in the receiver array and left-hand circular polarization in the transmitter array, have been selected to enhance the isolation between the two arrays.

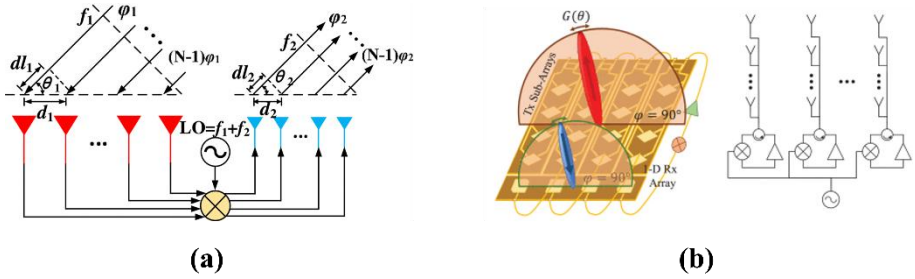

Fig. 14. (a) schematic of dual-frequency RDA [33], (b) schematic of the circularly polarized RDA [34].

Then, the retrodirectivity concept has been also applied to other radiating systems: in [35] a Rotman lens designed as a retrodirective beamforming network for far-field WPT operating in Ka-band is presented. This solution enables beamforming without any change in the lens configuration or additional circuits, and also allows to track the location of a target once a beacon signal is received from it. In [36], the use of a retrodirective FDA to provide both angle and range focused beamforming capability for long-range wireless information and power transfer is proposed. The focused range-angle beampattern can be independently controlled through properly designing the transmit weighting vector or the frequency offsets among the array elements. A representation of the retrodirective FDA scheme is shown in Fig. 15(a).

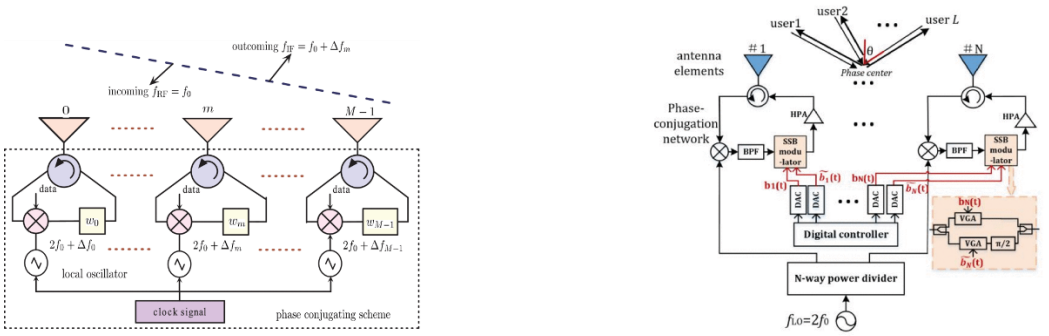

Fig. 15. (a) schematic of retrodirective FDA [36], (b) schematic of the retrodirective TMA in a multi-user scenario [37].

Furthermore, in [37] the issue of smart RF power beamforming in a multiuser WPT system is addressed. Specifically, it is proposed a two-stage communication/power transmission strategy based on the time modulation and retrodirective technique. Indeed, in a multi-user WPT scenario, the pilot signals emitted from the users are phase conjugated, time modulated using preprocessed rectangular pulses, and then retransmitted back to the users. Particularly, the multi-carrier modulating signals are optimally weighted to perform harmonics power beamforming. The configuration of the retrodirective TMA in a multi-user scenario is depicted in Fig. 15(b).

Several steps forward have been conducted on the retrodirective arrays, as highlighted in these recalled studies, however common problems of this technology remain. The main limitation of these radiating systems is the need for the interaction with active targets, that must send a pilot signal to the RF source: vice versa, the FDA and TMA solutions previously described can easily interact with totally passive targets. Additionally, retrodirective systems show a high implementation complexity due to the need for phase conjugation or sophisticated signal processing, and expensive components, especially when using analog or digital phase-conjugating circuitry (e.g., mixers, local oscillators, or digital signal processors for each antenna element). Moreover the signal processing involved in phase conjugation or digital retrodirectivity can introduce processing delays, which might be problematic for real-time applications.

On the other hand, the agile and reconfigurable capabilities of FDA and TMA solutions together with their affordable design allow to overcome these critical challenges, as detailed in the following sub-paragraphs.

4.1. Hardware design

The reduced complexity of the architecture is one of the key advantages of FDA and TMA with respect to phased arrays (PA) or Rotman Lens solutions. Indeed, a tough feeding network design is required for Rotman Lens [38], [39], whereas expensive components such as hybrid couplers and phase shifters are needed to design the beamforming network of a PA [40]. A schematic representation of these two systems is shown in Fig. 16(a) and Fig. 16(b), respectively.

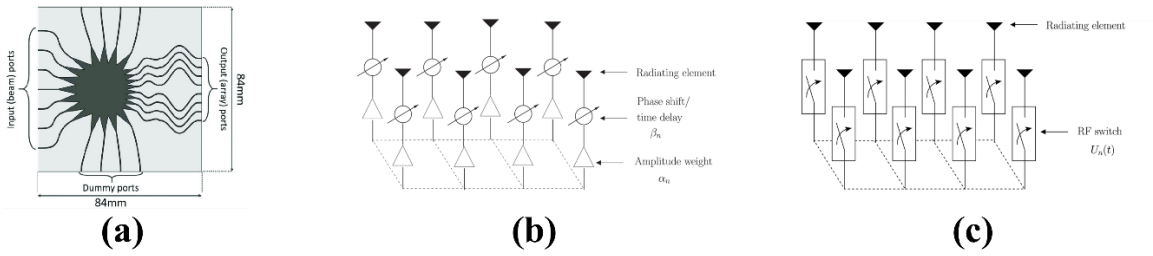

Fig. 16. (a) schematic of Rotman Lens design [35], (b) schematic of a regular phased array [40], (c) schematic of a TMA [40].

On the other hand, simple and less expensive switches are enough to manage pulsed FDA and TMA systems: each port of the array must be equipped with a switch to synthetize the corresponding control sequence, as shown in Fig. 16(c). For the FDA case a multi-tone generation is also mandatory, and it can be implemented through the use of a Software Defined Radio (SDR) as stated in [21].

4.2. Beam pattern reconfigurability

The experimental activity presented in [21] demonstrates the advanced beamforming capability of pulsed FDA in terms of both single- and multi-beam generation. Under this perspective, pulsed FDA exhibits superior performance with respect to TMA. A traditional TMA is able to produce harmonic radiations only in symmetric directions with respect to the carrier frequency, unless complex feeding strategies are employed [41-43], and this represents a main limitation of TMA. Other architectures such as Butler Matrix or Rotman Lens still have multi-beam capabilities, however their level of reconfigurability is limited by their design. For example, the use of digital phase shifters (that can be programmed) allows to cover a limited number of angles on which the beam can be steered. Vice versa, in a pulsed FDA system the delay τ of the control pulse can be selected on demand and modified in real time to point the single- or multi-beam in any target direction.

Overall, the low complexity and cost of the hardware combined with an advanced reconfigurability of the system are two key requirements for WPT applications, and currently pulsed FDA is the solution that most fulfil them.

4.3. Signal excitations

Further consideration about the operating regime of these radiating systems must be done. Differently from a PA that typically works with a single carrier CW signal, pulsed FDA and TMA operate with pulsed signals. In particular, the spectrum of a TMA signal is composed of a single carrier plus the corresponding harmonics, whereas in the pulsed FDA case there is a multi-carrier signal and the harmonics for each fundamental tone. Therefore, in these two cases there are more terms to be controlled to ensure a proper behavior of the system. In [22] it has been proved that pulsed FDA is an effective technique for WPT since the harmonic generation is favorably exploited, differently from other interference-aware applications. In terms of power transfer efficiency, the use of pulsed signals instead of CW can be an advantage or not depending on the application and on the power level to be rectified by a rectenna in reception [44]. In [21] an analysis of the rectenna performance, in terms of RF-to-dc conversion efficiency has been carried out for different types of signal excitations. The Harmonic Balance (HB) optimization, conducted in the available power range [-30 – -5] dBm, shows that pulsed FDA is slightly less effective than a PA in the lower power range. Vice versa, if the available power level exceeds -14 dBm, pulsed FDA outperforms both a standard CW FDA and a single tone CW (i.e. a phased array). These simulated results in terms of RF-to-dc efficiency (η_{RF-DC}) as a function of the available power P_{av} are shown in Fig 17.

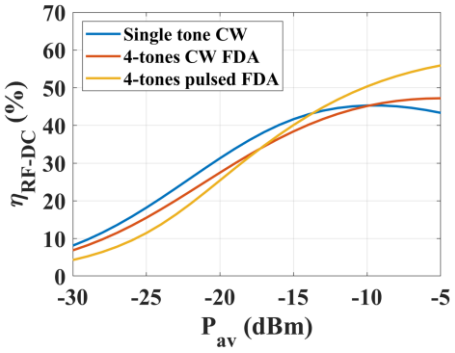

Fig. 17. RF-to-dc efficiency vs available power for different input excitations. [21]

Therefore, it has been proved that for certain power levels, having signals with high peak-to-average power ratio (PAPR), i.e. pulsed signals, guarantees better rectifying efficiency of the WPT system.

5. Practical limitations and future work

In this section, some practical aspects of the systems presented in this work are discussed, highlighting the strengths and weaknesses with respect to other solutions. Afterward, possible improvements and future developments of these technologies are presented.

5.1. Practical limitations

In order to meet the requirements of pulsed FDA and TMA systems in a real-world scenario, some important issues, such as power consumption and architecture scalability need to be addressed. The power consumption of pulsed FDA and of TMA is expected to be lower compared to a conventional phased array and to an active retrodirective array. This is because their architecture is simpler compared to the other two cases. As explained in section 4.1, it is enough to rely on RF switches at the antenna array ports to perform the modulation and control the beam pattern. These rather simple components introduce a lower power consumption with respect to phase shifters and hybrid couplers embedded in phase array architectures. Regarding retrodirective array solutions, common drawbacks of the active solution are the complexity and power consumption of their layout, since they require a phase-conjugating circuitry including mixers, circulators, power amplifiers. Currently, the main level of complexity of pulsed FDA is related to the signal generation. Indeed, a multi-tone excitation is required to ensure the proper frequency-diverse radiation. From a practical viewpoint, the use of a software-defined radio (SDR) is required to simultaneously generate independent and perfectly synchronized FDA signals. Whereas, a single-tone RF signal generator is enough to excite a phased array.

The scalability limitations in terms of number of radiating elements of pulsed FDA and TMA are mainly related to the hardware constraints. Indeed, from a theoretical viewpoint increasing the number of antennas is always possible and beneficial both for pulsed FDA and for TMA, since the directivity of the array increases and this is an added value to enhance the RF-to-RF efficiency of the WPT link. Moreover, for a TMA having a large number of radiating elements, thus of control ports, turns into a wider number of degrees of freedom to design and optimize the ON-OFF sequences that are used to control the array excitation. However, there are practical issues that limit the maximum number of radiating elements inside the array. Regarding pulsed FDA, since each antenna is radiating a signal (opportunely modulated) at a slightly different frequency from the others, the main hardware limitation is given by the maximum number of independent RF channels available in transmission. Latest and more advanced SDR solutions allow to reach a maximum of 16 parallel channels. This number could be extended by designing appropriate control boards to be interfaced at the output of the

SDR, but their design and complexity is not trivial. Moreover, the power consumption and losses of such extended solutions will increase and should be accounted in the overall system's efficiency. On the other hand, this limit on the signal generation is not affecting TMA systems, since they rely on a single RF carrier. The practical limitation of a TMA stands in the maximum number of RF switches and in the feeding network design to properly excite the array. Indeed, this control circuitry becomes complex and difficult to be managed as the number of antennas increases, and if more advanced array layouts (e.g. planar arrays) are envisaged. In general terms, for both solutions an increasing number of radiating elements should be pursued if affordable, in order to boost the directivity of the array. However, it is important to find the best trade-off between antenna array performance, low design complexity and limited losses in the control circuitry, to maximize the overall efficiency of the WPT system.

5.2. Future perspectives

Current and near-future works are oriented towards the applicability of these advanced architectures in real-world scenarios to address the challenges of the new wireless technologies. In this context, the combination of these radiating structures with efficient machine learning tools that are able to control in real-time the configuration of the array excitations, adapting them to the conditions of a dynamic wireless environment, is a crucial and demanding application. Few studies are orienting in this direction, by applying machine learning strategies to TMA. In [45] a machine learning approach applied to a two-element linear TMA for Direction of Arrival (DoA) estimation is proposed. The DoA estimation of the incoming signal from the source is formulated as a multiclassification problem. Then, the performance of this method are tested under various signal-to-noise ratio (SNR) conditions. A further example is shown in [46], where an AI-based optimization strategy is adopted for almost real-time reconfiguration of a circular array in realistic dynamic WPT scenarios. To test the system's reconfigurability, an optimization has been carried out in [46], whose numerical (continuous line) and experimental (dashed line) results are shown in Fig. 18. In this case, the goal is to keep the pattern at the fundamental frequency in the broadside direction, while steering the first and second order harmonics at $\vartheta = \pm 10°$ and $\vartheta = \pm 20°$ respectively, as shown in Fig. 18(b). To achieve this result, the TMA synthesis problem is formulated as a global optimization problem, with a dedicated cost function to be minimized. The optimized control sequences are shown in Fig. 18(a).

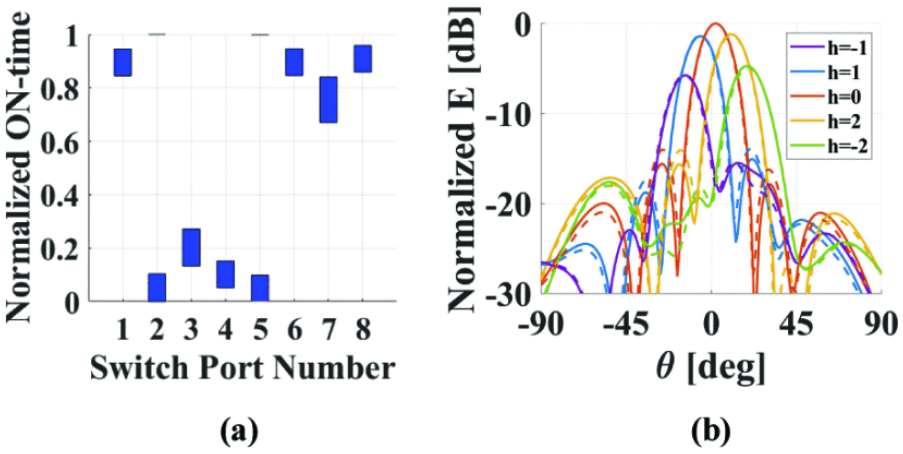

Fig. 18. Harmonic pattern of radial TMA: (a) optimized TMA control sequences, (b) first order harmonics at $\vartheta = \pm 10°$, second order harmonics at $\vartheta = \pm 20°$. Simulated curves are depicted with continuous lines, measured curves are depicted with dashed lines. [46]

Recently, in the framework of WPT for implantable medical devices, an investigation about RF power focusing using superoscillations has been presented in [47]. The use of radiating structures operating in the radiative

near-field region enables simultaneous beam steering and beam focusing, thus representing an attractive solution to develop efficient and highly reconfigurable WPT systems.

6. Conclusion

In this work FDA and TMA radiating solutions have been presented as two enabling technologies for current and future WPT systems. Some of the latest research activities on these topics have been recalled, trying to highlight the advantages carried by these array systems both in terms of design and in terms of their radiating performance: despite the complexity of their radiation mechanism, these systems offer quite a reduced hardware complexity if compared to more standard arrays (such as, phased- or retrodirective arrays). Preliminary measurement campaigns have demonstrated the feasibility of their usage as future RF showers for intentional transmission of energy.

Acknowledgment

This work was partly funded by the Italian Ministry of Education, University and Research (MIUR) within the framework of the PRIN 2022-INSIDENEXT (“INdoor Smart Illuminator for Device Energization and NEXtgeneration communicaTions”) and partially supported by the European Union - Next Generation EU under the Italian National Recovery and Resilience Plan (NRRP), Mission 4, Component 2, Investment 1.3, CUP J33C22002880001, partnership on “Telecommunications of the Future” (PE00000001 - program “RESTART”).

References

[1] P. Antonik, M. C. Wicks, H. D. Griffiths and C. J. Baker, "Range-dependent beamforming using element level waveform diversity," *2006 International Waveform Diversity & Design Conference*, Lihue, HI, USA, 2006, pp. 1-6, doi: 10.1109/WDD.2006.8321488.

[2] Jingjing Huang, Kin-Fai Tong, K. Woodbridge and C. Baker, "Frequency diverse array: Simulation and design," *2009 IEEE Radar Conference*, Pasadena, CA, USA, 2009, pp. 1-4, doi: 10.1109/RADAR.2009.4976998.

[3] Y. Liao, G. Zeng, Z. Luo and Q. H. Liu, "Time-Variance Analysis for Frequency-Diverse Array Beampatterns," in *IEEE Transactions on Antennas and Propagation*, vol. 71, no. 8, pp. 6558-6567, Aug. 2023, doi: 10.1109/TAP.2023.3281851.

[4] W. -Q. Wang and H. C. So, "Transmit Subaperturing for Range and Angle Estimation in Frequency Diverse Array Radar," in *IEEE Transactions on Signal Processing*, vol. 62, no. 8, pp. 2000-2011, April15, 2014, doi: 10.1109/TSP.2014.2305638.

[5] R. Çetiner, Ş. Demir and A. Hizal, "Range and angle measurement in a linear pulsed Frequency Diverse Array radar," *2017 IEEE Radar Conference (RadarConf)*, Seattle, WA, USA, 2017, pp. 0064-0067, doi: 10.1109/RADAR.2017.7944172.

[6] M. Secmen, S. Demir, A. Hizal and T. Eker, "Frequency Diverse Array Antenna with Periodic Time Modulated Pattern in Range and Angle," *2007 IEEE Radar Conference*, Waltham, MA, USA, 2007, pp. 427-430, doi: 10.1109/RADAR.2007.374254.

[7] P. Antonik, M. C. Wicks, H. D. Griffiths and C. J. Baker, "Frequency diverse array radars," *2006 IEEE Conference on Radar*, Verona, NY, USA, 2006, pp. 3 pp.-, doi: 10.1109/RADAR.2006.1631800.

[8] J. Xu, G. Liao, S. Zhu, L. Huang and H. C. So, "Joint Range and Angle Estimation Using MIMO Radar With Frequency Diverse Array," in *IEEE Transactions on Signal Processing*, vol. 63, no. 13, pp. 3396-3410, July1, 2015, doi: 10.1109/TSP.2015.2422680.

[9] P. F. Sammartino, C. J. Baker and H. D. Griffiths, "Frequency Diverse MIMO Techniques for Radar," in *IEEE Transactions on Aerospace and Electronic Systems*, vol. 49, no. 1, pp. 201-222, Jan. 2013, doi: 10.1109/TAES.2013.6404099.

[10] E. Fazzini, A. Costanzo and D. Masotti, "Wireless Power Transfer Procedure via Hybrid Frequency Diversity," *2021 51st European Microwave Conference (EuMC)*, London, United Kingdom, 2022, pp. 757-760, doi: 10.23919/EuMC50147.2022.9784280.

[11] W. Khan, I. M. Qureshi and S. Saeed, "Frequency Diverse Array Radar With Logarithmically Increasing Frequency Offset," in *IEEE Antennas and Wireless Propagation Letters*, vol. 14, pp. 499-502, 2015, doi: 10.1109/LAWP.2014.2368977.

[12] E. Fazzini, M. Shanawani, A. Costanzo and D. Masotti, "A Logarithmic Frequency-Diverse Array System for Precise Wireless Power Transfer," *2020 50th European Microwave Conference (EuMC)*, Utrecht, Netherlands, 2021, pp. 646-649, doi: 10.23919/EuMC48046.2021.9338242.

[13] A. Basit, I. M. Qureshi, W. Khan, S. u. Rehman and M. M. Khan, "Beam Pattern Synthesis for an FDA Radar with Hamming Window-Based Nonuniform Frequency Offset," in *IEEE Antennas and Wireless Propagation Letters*, vol. 16, pp. 2283-2286, 2017, doi: 10.1109/LAWP.2017.2714761.

[14] Y. Liao, W. -Q. Wang and Z. Zheng, "Frequency Diverse Array Beampattern Synthesis Using Symmetrical Logarithmic Frequency Offsets for Target Indication," in *IEEE Transactions on Antennas and Propagation*, vol. 67, no. 5, pp. 3505-3509, May 2019, doi: 10.1109/TAP.2019.2900353.

[15] A. -M. Yao, N. Anselmi and P. Rocca, "A novel planar frequency diverse array design approach for far-field wireless power transmission," *2017 IEEE International Symposium on Antennas and Propagation & USNC/URSI National Radio Science Meeting*, San Diego, CA, USA, 2017, pp. 1807-1808, doi: 10.1109/APUSNCURSINRSM.2017.8072946.

[16] A. Akkoç, E. Afacan and E. Yazgan, "Investigation of Planar Frequency Diverse Array Antenna in Concentric Circular Geometry," *2019 11th International Conference on Electrical and Electronics Engineering (ELECO)*, Bursa, Turkey, 2019, pp. 651-654, doi: 10.23919/ELECO47770.2019.8990521.

[17] A. Akkoc, E. Afacan and E. Yazgan, "Dot-Shaped 3D Range-Angle Dependent Beamforming With Discular Frequency Diverse Array," in *IEEE Transactions on Antennas and Propagation*, vol. 69, no. 10, pp. 6500-6508, Oct. 2021, doi: 10.1109/TAP.2021.3070128.

[18] E. Fazzini, A. B. Gok, A. Costanzo and D. Masotti, "Accurate Ranging Exploiting a 32-patch Frequency Diverse Array with Circular Symmetry," *2022 16th European Conference on Antennas and Propagation (EuCAP)*, Madrid, Spain, 2022, pp. 1-5, doi: 10.23919/EuCAP53622.2022.9768991.

[19] E. Fazzini, A. Costanzo and D. Masotti, "Range Selective Power Focusing with Time-controlled Bi-dimensional Frequency Diverse Arrays," *2021 IEEE Wireless Power Transfer Conference (WPTC)*, San Diego, CA, USA, 2021, pp. 1-4, doi: 10.1109/WPTC51349.2021.9458208.

[20] Y. Xu, X. Shi, J. Xu and P. Li, "Range-Angle-Dependent Beamforming of Pulsed Frequency Diverse Array," in *IEEE Transactions on Antennas and Propagation*, vol. 63, no. 7, pp. 3262-3267, July 2015, doi: 10.1109/TAP.2015.2423698.

[21] E. Fazzini, T. Tiberi, A. Costanzo and D. Masotti, "Enabling Multispot Wireless Power Transmission via Pulsed FDA for Simultaneous Dislocated Charging," in *IEEE Antennas and Wireless Propagation Letters*, vol. 23, no. 11, pp. 3847-3851, Nov. 2024, doi: 10.1109/LAWP.2024.3424222.

[22] T. Tiberi, E. Fazzini, A. Costanzo and D. Masotti, "Exploitation of Harmonic Generation in Time-Controlled Frequency-Diverse Arrays for WPT," in *IEEE Transactions on Antennas and Propagation*, vol. 72, no. 1, pp. 497-505, Jan. 2024, doi: 10.1109/TAP.2023.3324499.

[23] H. E. Shanks and R. W. Bickmore. 1959. FOUR-DIMENSIONAL ELECTROMAGNETIC RADIATORS. *Canadian Journal of Physics*. 37(3): 263-275.

[24] W. Kummer, A. Villeneuve, T. Fong and F. Terrio, "Ultra-low sidelobes from time-modulated arrays," in *IEEE Transactions on Antennas and Propagation*, vol. 11, no. 6, pp. 633-639, November 1963, doi: 10.1109/TAP.1963.1138102.

[25] L. Poli, P. Rocca, G. Oliveri and A. Massa, "Harmonic Beamforming in Time-Modulated Linear Arrays," in *IEEE Transactions on Antennas and Propagation*, vol. 59, no. 7, pp. 2538-2545, July 2011, doi: 10.1109/TAP.2011.2152323.

[26] Y. Tong and A. Tennant, "A Two-Channel Time Modulated Linear Array With Adaptive Beamforming," in *IEEE Transactions on Antennas and Propagation*, vol. 60, no. 1, pp. 141-147, Jan. 2012, doi: 10.1109/TAP.2011.2167936.

[27] E. Fazzini, T. Tiberi, A. Costanzo and D. Masotti, "Optimum Feeding Strategy for Agile Wireless Powering by Large, High-Directivity Time-Modulated Arrays," *2024 IEEE Wireless Power Technology Conference and Expo (WPTCE)*, Kyoto, Japan, 2024, pp. 142-145, doi: 10.1109/WPTCE59894.2024.10557357.

[28] A. Tennant and B. Chambers, "A Two-Element Time-Modulated Array With Direction-Finding Properties," in IEEE Antennas and Wireless Propagation Letters, vol. 6, pp. 64-65, 2007, doi: 10.1109/LAWP.2007.891953.

[29] C. He, X. Liang, Z. Li, J. Geng and R. Jin, "Direction Finding by Time-Modulated Array With Harmonic Characteristic Analysis," in *IEEE Antennas and Wireless Propagation Letters*, vol. 14, pp. 642-645, 2015, doi: 10.1109/LAWP.2014.2373432.

[30] C. He *et al*., "Direction Finding by Time-Modulated Linear Array," in *IEEE Transactions on Antennas and Propagation*, vol. 66, no. 7, pp. 3642-3652, July 2018, doi: 10.1109/TAP.2018.2835164.

[31] D. Masotti, A. Costanzo, M. Del Prete and V. Rizzoli, "Time-Modulation of Linear Arrays for Real-Time Reconfigurable Wireless Power Transmission," in *IEEE Transactions on Microwave Theory and Techniques*, vol. 64, no. 2, pp. 331-342, Feb. 2016, doi: 10.1109/TMTT.2015.2512275.

[32] T. Tiberi, L. Bastia, E. Fazzini, A. Costanzo and D. Masotti, "Agile Target Localization via Time-Modulation", presented at 2025 19th European Conference on Antennas and Propagation (EuCAP), Stockholm, Sweden, 2025.

[33] Y. Kang, X. Q. Lin, Y. Li and B. Wang, "Dual-Frequency Retrodirective Antenna Array With Wide Dynamic Range for Wireless Power Transfer," in IEEE Antennas and Wireless Propagation Letters, vol. 22, no. 2, pp. 427-431, Feb. 2023, doi: 10.1109/LAWP.2022.3215207.

[34] P. D. Hilario Re, S. K. Podilchak, S. A. Rotenberg, G. Goussetis and J. Lee, "Circularly Polarized Retrodirective Antenna Array for Wireless Power Transmission," in IEEE Transactions on Antennas and Propagation, vol. 68, no. 4, pp. 2743-2752, April 2020, doi: 10.1109/TAP.2019.2952011.

[35] H. Y. Hong, H. Soo Park and S. K. Hong, "Design of Rotman Lens for Far-field Wireless Power Transfer at Ka-band," 2020 IEEE Wireless Power Transfer Conference (WPTC), Seoul, Korea (South), 2020, pp. 109-111, doi: 10.1109/WPTC48563.2020.9295528.

[36] W. -Q. Wang, "Retrodirective Frequency Diverse Array Focusing for Wireless Information and Power Transfer," in IEEE Journal on Selected Areas in Communications, vol. 37, no. 1, pp. 61-73, Jan. 2019, doi: 10.1109/JSAC.2018.2872360.

[37] Y. -Q. Yang, H. Wang and Y. -X. Guo, "A Time-Modulated Array With Digitally Preprocessed Rectangular Pulses for Wireless Power Transmission," in IEEE Transactions on Antennas and Propagation, vol. 68, no. 4, pp. 3283-3288, April 2020, doi: 10.1109/TAP.2019.2930135.

[38] N. Jastram and D. S. Filipovic, "Wideband multibeam millimeter wave arrays," *2014 IEEE Antennas and Propagation Society International Symposium (APSURSI)*, Memphis, TN, USA, 2014, pp. 741-742, doi: 10.1109/APS.2014.6904700.

[39] I. -T. Chen, C. A. Lynch, A. Eid, J. G. D. Hester, K. Zeng and M. M. Tentzeris, "Additively Manufactured Semipassive Rotman Lens-Based RIS-Assisted mmID Tag System for Beyond-5G Wireless Networks in Complex Environments," in *IEEE Transactions on Microwave Theory and Techniques*, vol. 73, no. 1, pp. 650-660, Jan. 2025, doi: 10.1109/TMTT.2024.3422386.

[40] P. Rocca, G. Oliveri, R. J. Mailloux and A. Massa, "Unconventional Phased Array Architectures and Design Methodologies—A Review," in *Proceedings of the IEEE*, vol. 104, no. 3, pp. 544-560, March 2016, doi: 10.1109/JPROC.2015.2512389.

[41] A. -M. Yao, W. Wu and D. -G. Fang, "Single-Sideband Time-Modulated Phased Array," in *IEEE Transactions on Antennas and Propagation*, vol. 63, no. 5, pp. 1957-1968, May 2015, doi: 10.1109/TAP.2015.2406890.

[42] Q. Chen, J. -D. Zhang, W. Wu and D. -G. Fang, "Single-Sideband Time-Modulated Phased Array With S-Step Waveform," in *IEEE Antennas and Wireless Propagation Letters*, vol. 19, no. 11, pp. 1867-1871, Nov. 2020, doi: 10.1109/LAWP.2020.2989477.

[43] Q. Chen, J. -D. Zhang, W. Wu and D. -G. Fang, "Enhanced Single-Sideband Time-Modulated Phased Array With Lower Sideband Level and Loss," in *IEEE Transactions on Antennas and Propagation*, vol. 68, no. 1, pp. 275-286, Jan. 2020, doi: 10.1109/TAP.2019.2938711.

[44] A. Boaventura, D. Belo, R. Fernandes, A. Collado, A. Georgiadis and N. B. Carvalho, "Boosting the Efficiency: Unconventional Waveform Design for Efficient Wireless Power Transfer," in *IEEE Microwave Magazine*, vol. 16, no. 3, pp. 87-96, April 2015, doi: 10.1109/MMM.2014.2388332.

[45] M. R. Mathew, A. P, D. Das Krishna and P. Murali Krishna, "Direction Finding in Time Modulated Linear Arrays Using Supervised Machine Learning," *2024 IEEE International Conference on Signal Processing, Informatics, Communication and Energy Systems (SPICES)*, KOTTAYAM, India, 2024, pp. 1-5, doi: 10.1109/SPICES62143.2024.10779930.

[46] L. Bastia, T. Tiberi, L. Poli, P. Rocca, A. Costanzo and D. Masotti, "Agile microwave WPT exploiting circular array with optimized time-modulated excitations," *2025 IEEE Wireless Power Technology Conference and Expo (WPTCE)*, Rome, Italy, 2025, pp. 1-5, doi: 10.1109/WPTCE62521.2025.11062089.

[47] M. Abdolrazzaghi, R. Genov and G. V. Eleftheriades, "Subwavelength-Scale Focused Wireless Powering of Implantable Medical Devices by Superoscillations," in *IEEE Transactions on Microwave Theory and Techniques*, doi: 10.1109/TMTT.2025.3568486.